Available online at www.sciencedirect.com
ScienceDirect
Journal of the European Ceramic Society 29 (2009) 925–929
www.elsevier.com/locate/jeurceramsoc

Shaping of advanced ceramics: The case of composite electrodes for lithium batteries

E. Ligneel, B. Lestriez*, A. Hudhomme, D. Guyomard

CNRS UMR 6502 Institut des Matériaux Jean Rouxel, 2 rue de la Houssinière, B.P. 32229, 44322 Nantes Cedex 3, France

Available online 28 August 2008

Abstract

Composite electrodes for electrochemical energy storage systems, such as lithium batteries, are mixtures of a ceramic powder, an electronic conducting agent, often carbon black, and a polymeric binder. Such a complex medium must provide efficient transport of electrons and ions from the current collector/electrode and electrolyte/electrode interfaces, respectively, to the grain surface of the ceramic. It seems quite obvious that the morphology within the composite electrode should have an influence on the electrode performance. However, such an issue has never been studied yet. Here we study composite electrodes prepared by the tape casting method, with the purpose to gain better understanding of the relationships between: the suspension properties, the morphology within the dried composite electrode, and the resulting electrochemical properties.

Keywords: Electrode; Lithium battery; Electrical properties; Suspension; Carbon black; Binder

1. Introduction

Most studies in the field of rechargeable batteries deal with the search for new structures of active electrode materials or with the optimization of already known compositions. But the active material of a battery cannot function by itself as an electrode. The electrode is in fact a very complex medium that needs to bring efficiently the ionic reactants and the electrons to the surface of the active material particles. In the field of lithium batteries, this composite electrode needs to possess mixed conductivity with both lithium ion and electron conductivity. Such a complex medium is generally obtained by mixing together the active material grains with non-electroactive additives such as a very fine powder of carbon black (CB) and a polymeric binder. The CB additive is supposed to ensure electronic percolation within the composite electrode. The binder additive brings its mechanical strength to the electrode. This dry composite material is then impregnated by the liquid electrolyte during the assembly of the battery.

It seems quite obvious that the morphology within the composite should have an influence on the electrode performance. However, such an issue is a research area that has never been studied yet.

Here we study lithium trivanadate based electrodes. $Li_{1.1}V_3O_8$, which offers a theoretical capacity of 360 mAh/g, has been investigated as a very promising positive electrode material over the past two decades.[1,2] However, the experimental capacity remained much lower than the theoretical value. It has long been of only 150 mAh/g with standard-type (poly(vinylidene fluoride) binder) composite electrode. Recent results show that using a plasticized polyethylene oxide or poly(methylmethacrylate) (PMMA) binder with the ethylene carbonate-propylene carbonate (EC + PC) electrolyte solvent or the liquid electrolyte itself leads to a room temperature cycling capacity of 280 mAh/g, and 330 mAh/g at 55 °C.[3–5] The fairly low cycling capacity usually obtained for $Li_{1.1}V_3O_8$ was thus due to inefficient environment in the electrode. The goal of the present work is to study the electrode processing steps with the purpose to gain better understanding of the relationships between: the non-aqueous suspension properties, the morphology within the dried tape-cast electrode, and the resulting electrochemical properties.

2. Experimental procedure

2.1. Materials

A home-synthesized $Li_{1.1}V_3O_8$ (at 580 °C)[6] was used as the active material, and carbon black (Super-P, noted CB, ERACHEM), as a conductive agent. The binder was

* Corresponding author. Tel.: +33 2 40 37 39 32; fax: +33 2 40 37 39 95.
E-mail address: Bernard.lestriez@cnrs-imn.fr (B. Lestriez).

0955-2219/$ – see front matter © 2008 Elsevier Ltd. All rights reserved.
doi:10.1016/j.jeurceramsoc.2008.07.007

pure PMMA (Mw = 996,000 g mol^{-1}, Aldrich) or plasticized PMMA/EC + PC. Battery-grade chemicals such as ethylene carbonate (noted EC) (Aldrich), propylene carbonate (noted PC) (Aldrich), tetrahydrofuran (THF) (purity > 99.95%, SDS), and lithium bistrifluorosulfonimide (LiTFSI, 3 M) were all used as received.

The composite electrodes were prepared by following a classical solvent route where THF was used as the dispersing medium. The $Li_{1.1}V_3O_8$ and CB powders were dispersed in the binder solution to form a suspension using a magnetic stirrer for 12 h. The solvent concentration, expressed in milliliter per milligram of dry electrode, was 0.006 ml/mg. The dry electrode was constituted of 73% (w/w) of $Li_{1.1}V_3O_8$, 8% (w/w) of CB and 19% (w/w) of PMMA. When the binder was plasticized, the liquid additive EC + PC represents 20% (w/w) of the dry electrode. The suspension was then spread on aluminium disks (1 cm^2) for electrochemical measurements or on adapted supports. These composite films were dried at room temperature for 2 h to evaporate the solvent, dried further under vacuum at 50 °C for 1 h. For electrochemical measurements they were then transferred under dry argon atmosphere in a glove box (H_2O < 1 ppm) for battery assembly.

2.2. Properties of the electrode tape-cast films

For electrochemical measurements, two-electrode Swagelok test cells[7] using the composite electrode, a porous paper soaked with electrolyte as the separator, and metallic lithium as the negative electrode, were assembled in a glove box. A mixture of EC/PC (1:1, w/w) containing 1 M LiTFSI was used as liquid electrolyte. All voltages given in the text are reported vs. Li^+/Li. Cell cycling was performed at 20 °C, monitored by a VMP^{TM} system in galvanostatic mode. The voltage range used was 3.3–2 V. The composite electrodes were studied at the same current rate, calculated by considering that the insertion of one lithium per formula unit lasted 2.5 h in discharge and 5 h in charge.Two-electrode measurements of the electronic conductivity were performed by sandwiching disks of composite tapes between current collectors under an applied pressure of 90 MPa. The impedance of the samples was measured at 25 °C by means of a frequency response analyzer (Solartron 1260) in 1 Hz–2 MHz frequency range.

Scanning electron microscopy (SEM) imaging was performed on gold–palladium sputtered samples using a JEOL JSM 6400F apparatus. Cryogenic fracture was used to image the section of the samples.

BET surface area measurements (ASAP 2010 micromeritrics) were performed with nitrogen adsorption after outgassing the samples at 100 °C for 12 h under vacuum. In these experimental conditions, the BET surface area of neat CB and neat $Li_{1.1}V_3O_8$ was measured to be 70 and 0.5 m^2/g respectively.

2.3. Characteristics of the electrode suspensions

Rheological properties were measured at 25 °C under steady shear between 1000 and 1 s^{-1}. We used a controlled rate viscosimeter (VT550 HAAKE) equipped with a standard Couette cell that contains the sample in a 0.9 mm concentric cylindrical gap between a cup, 12.45 mm diameter, and a bob, 10.65 mm diameter and 31.95 mm length. Temperature was controlled by a circulating water bath, typically to within 25 ± 0.2 °C.

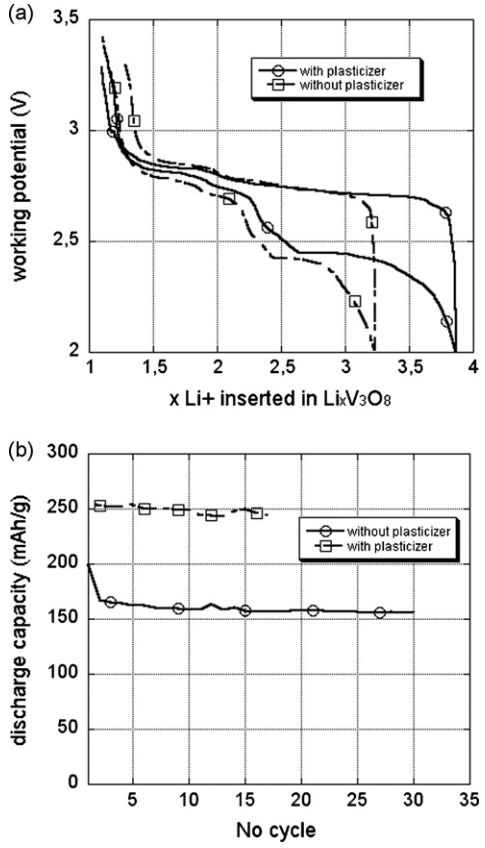

Fig. 1. (a) Voltage profile (discharge) vs. lithium composition at first cycle for cells made with a non-plasticized and an EC + PC plasticized electrode. (b) Discharge capacity vs. cycle number at room temperature for the same cells.

The CB particle-size distribution in the suspension was analysed by low angle laser light scattering (laser granulometry, Beckman Coulter LS 230). The optical model was based on the Mie theory and the value that was used for the real part of the CB refractive index of CB was $n = 1.95$.[8]

The drying kinetics of the electrode suspension was followed with gravimetric analysis, through monitoring weight percentage loss as a function of time at a temperature of 25 °C.

Settling rates were determined for electrode suspensions poured into closed tubes. The fall of the interfacial plane between the electrode slurry and the clear supernatant was monitored as a function of time at a temperature of 25 °C.

3. Results and discussion

3.1. Properties of the tape-cast electrode films

Electrochemical performance is shown in Fig. 1. Voltage profile vs. lithium composition at first cycle is shown in Fig. 1a. Cycle performance is given as the discharge capacity per mass of active material vs. cycle number in Fig. 1b. For the

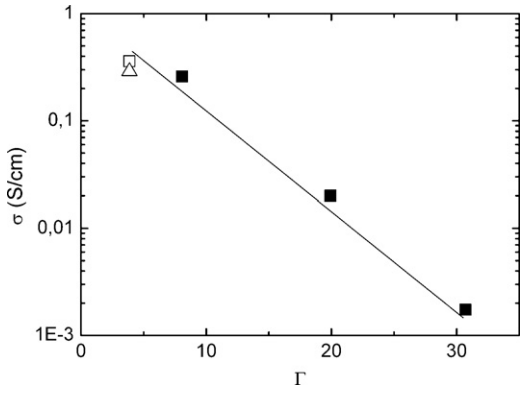

Fig. 2. Electronic conductivity vs. the PMMA to CB concentration ratio Γ for the non-plasticized (-△-) and the EC + PC plasticized (-□-) electrode, and model CB/PMMA composite mixtures (-▲-).

non-plasticized electrode whose binder was PMMA, 2.2 lithium were reversibly intercalated and a further cycling capacity of 160 mAh/g was displayed. Adding the plasticizer produced a net increase of cycle performance. Indeed, 2.9 lithium were intercalated and the discharge capacity remained stable upon cycling at 250 mAh/g for the plasticized electrode. The larger discharge capacity can be interpreted as coming from more numerous AM grains wired to the electrical circuits. Because the experimental discharge rates are low, ionic conductivity must be a second-rate factor to explain these results.

The electronic conductivity was measured on the dry composite electrodes and model composite mixtures of CB and PMMA in which the PMMA to the CB concentration ratio, Γ, was varied. $\Gamma = \phi_{PMMA}/\phi_{CB}$, where ϕ_i is the volume fraction of the i constituent. In Fig. 2, conductivity plots for all the composites are shown on a log scale as a function of Γ. A unique linear trend that obeys the equation

$$\log \sigma = \frac{-a\phi_{PMMA}}{\phi_{CB}} + b \quad (1)$$

is obtained, roughly independent of the $Li_{1.1}V_3O_8$ and of the EC + PC plasticizer presence. The combination of percolation theory and interparticle tunneling conduction describes fairly well the electrical behavior of CB composite.[9] In these systems, at the macroscopic scale, the conduction paths form a well-defined percolation-like network, and at the microscopic scale, the interparticle electrical contacts are due to tunneling of the electrons through the insulating polymer layers adsorbed in between the conducting particles. For a very narrow distribution of the width w of the insulating gaps, the composite conductivity can be described by the behavior of a single tunnel junction and the electrical conductivity is expected to vary like

$$\log \sigma \propto -w \quad (2)$$

For a random distribution of particles, then the mean average distance between particles has been shown to be proportional to $\phi_{CB}^{-1/3}$, thus providing a dependence of the conductivity as $\log \sigma \sim (\phi_{CB}^{-1/3})$.[10,11] Here, the combination of Eqs. (1) and (2) gives

$$w \propto \frac{\phi_{PMMA}}{\phi_{CB}} \quad (3)$$

which suggests that the CB network is highly structured with a non-random distribution of the CB particles and a very narrow distribution of the thickness of the polymer layer adsorbed in between.

SEM observation of the section of the non-plasticized electrode is shown in Fig. 3. The $Li_{1.1}V_3O_8$ grains appear homogeneously distributed in a dense 3D network of CB/PMMA. No visual difference in the morphology of the plasticized electrode was detected. However, the BET surface area increased from 5 to 7 m^2/g when adding the EC + PC plasticizer, which may be due to a finer CB distribution into the plasticized electrode. In a composite electrode, the electronic charge transfer efficiency depends on the quality of the electronic wiring of the AM grains. In the case of the plasticized electrode, the finer CB distribution probably results to more numerous electrical contacts at the CB/$Li_{1.1}V_3O_8$ interface thus leading to more efficient electronic charge transfer.

In summary, adding the plasticizer EC + PC in the binder composition clearly produces a net increase of the discharge capacity whose origin is neither an increase of the ionic conductivity, nor an increase of the electronic conductivity of the PMMA/CB network. Results seem to show that it may come from more efficient electronic charge transfer resulting from a finer CB distribution within the electrode film.

3.2. Characteristics of the electrode suspensions

The CB particle-size distribution in the suspension ranges from 10 μm to less than 0.3 μm, Fig. 4. The number frequency shows that the more numerous CB particles have a diameter that is less than 1 μm. However, the volume frequency shows that most of the CB volume consists of a minority of larger particles whose mean diameter is 5 μm. This suggests that more energetic mechanical means are necessary to give a better division of CB. Moreover, Fig. 4 shows that adding the plasticizer yields a finer dispersion of the CB with a higher number of small particles.

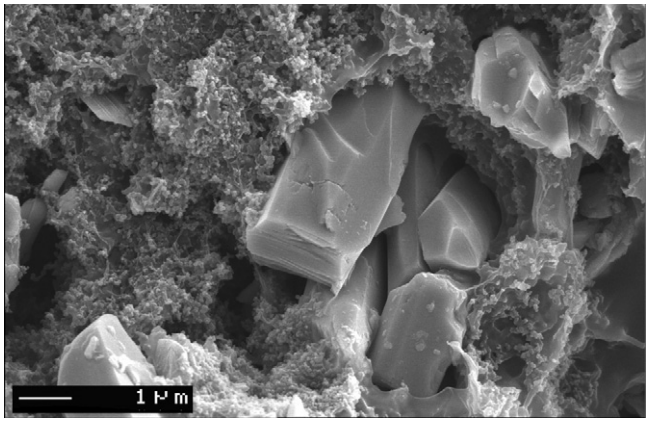

Fig. 3. SEM image of the non-plasticized electrode.

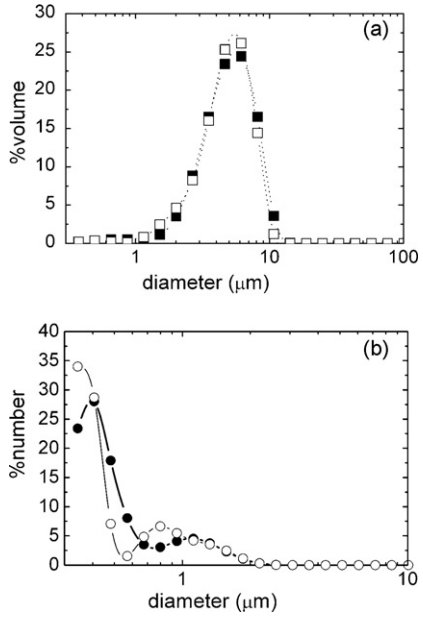

Fig. 4. CB particle-size distribution, (a) %volume and (b) %number in a non-plasticized (-■- and -●-) and EC + PC plasticized (-□- and -◯-) suspensions of CB/PMMA.

CB primary aggregates, which have an average diameter of 100–300 nm, consist of the smallest dispersible particles. They further give larger secondary structures of aggregates held together with only physical bonds, often-denoted agglomerates.[12] Two main forces oppose when dispersing the CB powder into the solvent: the hydrodynamic shear stress and the van der Waals attractive force. Three mechanisms transform CB agglomerates into a dispersion of aggregates.[13] Rupture occurs when the hydrodynamic shear stress exceeds the agglomerate cohesive stress. Collision is an active mechanism as soon as the concentration is large. Erosion is a much slower process than rupture that occurs at a smaller applied hydrodynamic stress. It consists of the removal of small particles or aggregates from the surface of the agglomerate. The particle-size distribution shown in Fig. 4 seems to result from an erosion mechanism.

The effective Hamaker constant A_{eff} can give an insight to the strength of the long-range interaction due to apolar van der Waals forces that attract two particles immersed in a fluid.[14] The constant A_{eff} is determined by the individual Hamaker constants (A_{ii}) of the two media and may be related to the dispersive (apolar) component of the individual surface tensions (γ_i^{d})[14]

$$A_{\text{eff}} = 2.1 \times 10^{-21}\left(\sqrt{\gamma_1^{\text{d}}} - \sqrt{\gamma_2^{\text{d}}}\right)^2 \quad (4)$$

Let us now calculate the effective Hamaker constant A_{eff} for interaction of CB in THF or EC + PC. We use $\gamma_{\text{CB}}^{\text{d}} = 66\,\text{mN/m}$,[15] $\gamma_{\text{THF}}^{\text{d}} = 21.2\,\text{mN/m}$ and $\gamma_{\text{EC+PC}}^{\text{d}} = 28.5\,\text{mN/m}$.[16] On the basis of these values, we compute A_{eff} for CB in THF to be 26×10^{-21} J, and A_{eff} for CB in EC + PC to be 16.3×10^{-21} J. These values are in agreement with literature[14,17] and show that the van der Waals interactions between CB aggregates are weakened when EC + PC is added to the suspension, thus explaining the finer CB dispersion.

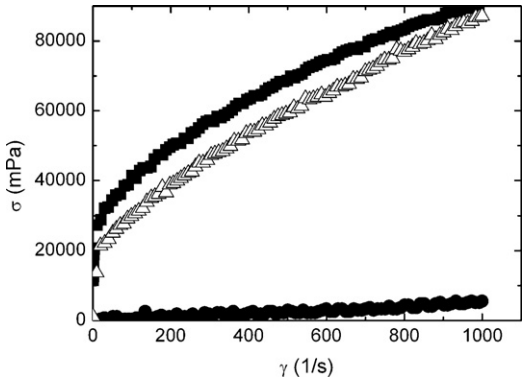

Fig. 5. Evolution of the shear stress with the shear rate for different solvent concentrations of the non-plasticized (-●- 0.010 ml/mg, -■- 0.003 ml/mg) and EC + PC plasticized suspensions, (-△- 0.003 ml/mg).

The rheological behavior of the electrode suspensions was studied for different solvent concentrations, Fig. 5. The less concentrated suspension (0.010 ml/mg) exhibits a Newtonian behavior while the more concentrated one (0.003 ml/mg) exhibits a yield stress as well as shear thinning behavior. This behavior is typical of weakly flocculated systems. The relative high $Li_{1,1}V_3O_8$ + CB volume fraction and the presence of attractive forces between the particles lead to a connectivity throughout the system, giving rise to a weak network. The yield stress is a manifestation of the network structure present in the system and signifies the minimum stress required to induce sample flow. Upon the application of a shear rate the network is progressively broken down into individual particles and the viscosity is continuously lowered. A decrease in the interaction energy between particles when the plasticizer is added to the suspension is apparent in the decreased yield stress.

Finally, the drying mechanism was approached through a study of its kinetics, Fig. 6. The variation of the solvent concentration vs. time shows two different periods. First, the solvent loss follows a linear stage. The second stage is characterized by a decreasing rate of drying. In agreement with literature,[18] we found that in the constant rate period the surface remains saturated with the solvent. Fig. 6 gives a comparison between the evolution as a function of time of: (i) the tape casting suspension

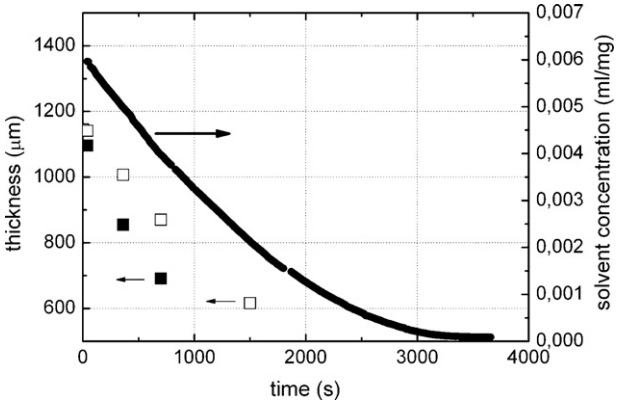

Fig. 6. Evolution as a function of the time of the solvent concentration (-●-), the surface height (-□-), and the position of the top surface particle that settle (-■-), of a tape casting suspension containing the EC + PC plasticized electrode.

surface height (calculated by considering that the volume variation of the tape corresponds to the solvent volume evaporated), and (ii) the position of the top surface particles that settle (calculated from independent settling rates measurements as described in the experimental section). The settling rate is slightly higher than the falling rate of the position of the tape casting suspension surface. The settling rate decreases to zero when the solvent concentration reaches 0.003 ml/mg. Rheological measurements show that near to this value, the suspension flocculates, giving rise to the CB/PMMA conducting network and creating the CB/$Li_{1.1}V_3O_8$ contacts. From this point, the shrinkage of the tape casting suspension becomes governed by the balance between capillary pressure exerted by the liquid in the pore and the elastic modulus of the structure. Later on, when this last contribution comes to prevail, the shrinkage stops. This point corresponds to the apparition of porosity in the film.

4. Conclusion

The morphology within the dried tape-cast electrode and the resulting electrical properties and electrochemical performance depend on the suspension characteristics and drying mechanism. The CB/CB and CB/LiV_3O_8 electrical contacts form during drying under zero shear stress. When the solvent concentration decreases the suspension flocculates. It results a very narrow distribution of the thickness of the polymer layers adsorbed in between the different particles and the quality of the electrical contacts depends on the concentration ratio ϕ_{PMMA}/ϕ_{CB}. The quantity of the CB/LiV_3O_8 electrical contacts depends on the CB particle-size distribution in the suspension. Adjusting solvent characteristics and the mechanical means used for preparing the suspension can be used to control this parameter.

Acknowledgments

We gratefully thank M. Suchaux and B. Corraze for the electrical measurements.

References

1. Panero, S., Pasquali, M. and Pistoia, G., *J. Electrochem. Soc.*, 1983, **130**, 1225.
2. Bonino, F., Ottaviani, M., Scrosati, B. and Pistoia, G., *J. Electrochem. Soc.*, 1988, **135**, 12.
3. Guy, D., Lestriez, B. and Guyomard, D., *Adv. Mater. (Weinheim, Ger)*, 2004, **16**, 553–557.
4. Guy, D., Lestriez, B., Bouchet, R., Gaudefroy, V. and Guyomard, D., *Electrochem. Solid-State Lett.*, 2005, **8**, A17–A21.
5. Ligneel, E., Lestriez, B., Richard, O. and Guyomard, D., *J. Phys. Chem. Solids*, 2006, **67**, 1275–1280.
6. Jouanneau, S., Verbaere, A., Lascaud, S. and Guyomard, D., *Solid State Ionics*, 2006, **177**, 311–315.
7. Leroux, F., Guyomard, D. and Piffard, Y., *Solid State Ionics*, 1995, **80**, 30.
8. Kattawar, G. W. and Hood, D. A., *Appl. Opt.*, 1976, **15**, 1996–1999.
9. Guy, D., Lestriez, B., Bouchet, R. and Guyomard, D., *J. Electrochem. Soc.*, 2006, **153**, A679–A688.
10. Boettger, H. and Bryksin, U. V., *Hopping Conduction in Solids*. VCH, Weinheim, 1985, p. 108, 148.
11. Ezquerra, T. A., Connor, M. T., Roy, S., Kulescza, M., Fernandes-Nascimento, J. and Balta-Calleja, F. J., *Compos. Sci. Technol.*, 2001, **61**, 903.
12. Leblanc, J. L., *Prog. Polym. Sci.*, 2002, **27**, 627–687.
13. Seyvet, O. and Navard, P., *J. Appl. Sci.*, 2001, **80**, 1627–1629.
14. Israelachvili, J. N., *Intermolecular and Surface Forces*. Academic Press, London, 1992.
15. Gonzalez-Garcia, C. M., Gonzalez-Martin, M. L., Gomez-Serrano, V., Bruque, J. M. and Labajos-Broncano, L., *Langmuir*, 2000, **16**, 3950–3956.
16. Ligneel, E., PhD, University of Nantes, 2006.
17. Georges, E., Georges, J. M. and Hollinger, S., *Langmuir*, 1997, **13**, 3454–3463.
18. Chotard, T., Quet, A., Ersen, A. and Smith, A., *J. Eur. Ceram. Soc.*, 2006, **26**, 1075–1084.